Journal of Thermal Analysis and Calorimetry
https://doi.org/10.1007/s10973-025-14948-5

Application of a skin calorimeter to study local heat loss during exercise

Pedro Jesús Rodríguez de Rivera[1] · Miriam Rodríguez de Rivera[2] · Fabiola Socorro[1] · Manuel Rodríguez de Rivera[1]

Received: 2 August 2025 / Accepted: 9 October 2025

Abstract
The evaluation of local heat loss during exercise provides relevant information on muscle activity and thermoregulatory mechanisms. In this study, a custom-designed skin calorimeter was used to measure heat loss over active muscles during moderate exercise. The device incorporates a thermopile and a thermostat, enabling precise thermal control and reliable heat flux estimation through a previously validated thermal model. We propose a method to characterize muscle's thermal response using a personalized transfer function (TF) that relates the mechanical power developed by the subject to the localized heat flux. Experiments were conducted on a healthy male subject, performing exercise at 80 W on a stepper. The heat flux was measured at the rectus femoris, under different thermostat temperatures. The resulting TFs showed consistent dynamic behavior, with sensitivities and time constants that support quantification of the muscle's thermal response. These findings support the feasibility of using skin calorimetry to non-invasively model muscle heat dynamics during exercise. This approach establishes a solid basis for future clinical applications.

Keywords Direct calorimetry · Non-differential calorimetry · Skin heat flux · Sport medicine sensors

Introduction

During whole-body exercise, the mechanical work performed by a subject can reach up to 25% of the metabolic energy measured by indirect calorimetry [1]. This percentage depends on the individual, the type and intensity of exercise, and environmental conditions, among other factors [2]. Some authors refer to this percentage as exercise efficiency, which in trained subjects is typically around 20% for workloads of about 200 W [3]. A rapid rise in muscle temperature shortens time to exhaustion, while a slower rise delays fatigue [4]. Therefore, the time evolution of muscle heat flux plays a key role in exercise performance. Exercise intensity is often monitored through several methods, with heart rate being the most accessible. Open-circuit indirect calorimetry is widely recognized as the reference method for estimating whole-body energy expenditure via pulmonary gas exchange [5, 6]. It offers high accuracy and reproducibility but provides only global values and requires bulky and specialized equipment, which limits its use in non-clinical settings. Indirect calorimetry offers valuable global assessment, but do not capture local thermal responses.

Several techniques have been widely used to investigate thermal behavior at a localized level. Infrared thermography has been used to characterize heat loss both at rest and during exercise [7], as well as to assess local pathologies and inflammatory processes [8]. Near-infrared spectroscopy is able to monitor oxygen saturation and perfusion, giving a functional view of the oxygen balance [9]. Heat flux sensors directly measure local heat loss and allows core temperature estimation [10]. However, their accuracy is limited by ambient conditions, sensor-induced disturbances, and alterations in convection and radiation [11]. Intramuscular thermistors are invasive, but effective for assessing thermal states at depths unreachable by other technologies [12].

In this context, skin calorimetry has emerged. Although localized heat flux has been measured in previous studies [13], its assessment during exercise has only recently been explored [14]. For this reason, the clinical application of this technique is still under development, requiring standardized

✉ Pedro Jesús Rodríguez de Rivera
pedro.rguezderivera@ulpgc.es

[1] Department of Physics, Universidad de Las Palmas de Gran Canaria (ULPGC), Las Palmas de Gran Canaria, Spain

[2] Cardiology Service, Hospital Universitario Marqués de Valdecilla, Santander, Spain

Published online: 03 November 2025

protocols and broader validation. This work aims to contribute additional evidence by presenting a mathematical model based on a subject—and muscle—specific transfer function (TF), to characterize muscle heat flux dynamics during moderate exercise, moving toward a more robust and personalized clinical use. This TF is consistent with the Pennes bio-heat equation [15], as the number of poles aligns with findings from several studies showing that two exponential terms are sufficient to describe heating and cooling processes [16–18]. As a novel contribution, the proposed TF includes a double real pole that allows the characterization of the transients in heating and cooling dynamics [4].

The manuscript is structured as follows: Materials and Methods section describes the calorimeter, the heat flux measurement, its operating modes, and the experimental protocol. The following section presents the analysis of local heat loss during exercise, introducing the proposed TF approach and the simulation results.

Materials and methods

Skin calorimeter and heat flux measurement

The skin calorimeter used in this study consists of a thermopile placed between a measurement plate and a programmable thermostat. The device is applied to a localized area of the skin using a custom holding system, covering a measurement surface of 2×2 cm^2. The thermostat incorporates a Peltier-based cooling system that enables precise temperature control over a wide range of ambient conditions. At typical room temperatures (18–30 °C), it can be programmed with a resolution of 10 mK, either to maintain a constant value (thermostat at 15–40 °C) or to apply linear temperature ramps [13]. Additionally, the calorimeter includes lateral thermal insulation to minimize external disturbances from conduction, convection, and radiation.

The thermal model of the calorimeter is based on the relationship between the heat flux transmitted from the skin to the calorimeter, and a set of measured and controlled variables. These include the thermopile signal, the thermostat temperature, the power dissipated in the thermostat, the current supplied to the Peltier module, and the ambient temperature. This model has been validated through Joule calibration tests under various operation conditions, ensuring the reliability of the heat flux estimations derived from the measurements [14]. The model considers two domains with heat capacities C_1 (skin) and C_2 (thermostat). These domains are thermally connected through the measurement thermopile, characterized by a thermal conductance P_{12} and a Seebeck coefficient k. Both domains are connected to the environment through conductances P_1 and P_2. Assuming power inputs W_1 and W_2 in each domain, the model equations can be expressed as:

$$\begin{aligned} W_1 &= C_1\frac{\mathrm{d}T_1}{\mathrm{d}t} + P_{12}\left(T_1 - T_2\right) + P_1(T_1 - T_{01}) \\ W_2 &= C_2\frac{\mathrm{d}T_2}{\mathrm{d}t} + P_{12}\left(T_2 - T_1\right) + P_2(T_2 - T_{02}) \end{aligned} \tag{1}$$

where T_1 and T_2 are the temperatures of each domain. T_{01} represents the local ambient temperature surrounding the calorimeter, which differs from the global ambient temperature (T_{room}) due to proximity to the skin, the heat dissipation from the cooling thermopile via the heat sink, and the movement of the calorimeter during exercise. T_{02} corresponds to the cold-side temperature provided by the Peltier module. The calorimetric signal and the external temperatures can be expressed by the following relations:

$$\begin{aligned} y &= k\left(T_1 - T_2\right) \\ T_{01} &= T_{\mathrm{room}} + \alpha I_{\mathrm{pel}} \\ T_{02} &= T_{\mathrm{room}} + \beta I_{\mathrm{pel}} \end{aligned} \tag{2}$$

From Eq. 1 and Eq. 2, and for a constant thermostat temperature T_2, we can deduce an expression for the heat flux estimation W_1 as a function of the calorimetric signal (y), the Peltier current (I_{pel}), and the thermostat power (W_2). The time constant τ_C is proportional to the heat capacity C_1, and ranges from 13 s (no sample) to 30 s (skin).

$$W_1 = a\left(y + \tau_C\frac{\mathrm{d}y}{\mathrm{d}t}\right) + b\cdot I_{\mathrm{pel}} + c\cdot W_2 \tag{3}$$

Table 1 lists the parameter values corresponding to Eq. 3 for the two skin calorimeters used in this study. These values were obtained through calibration procedures in which the calorimeter response was analyzed under varying thermostat temperatures, Peltier currents, and different Joule dissipations in the calibration resistor [19]. Under normal operating conditions, the resolution of the calorimetric signal provided by the thermopile is 0.3 mV, and the estimated resolution for the calculated heat flux is 5 mW.

Operating modes

The skin calorimeter operates in two modes. The first mode consists of applying a thermal excitation to the skin to determine its thermal properties. This excitation

Table 1 parameters of Eq. 3

Calorimeter	a /WV^{-1}	b /WA^{-1}	c /WW^{-1}
*S*1	7.0805	−2.8159	0.50877
*S*2	7.1708	−2.9348	0.52727

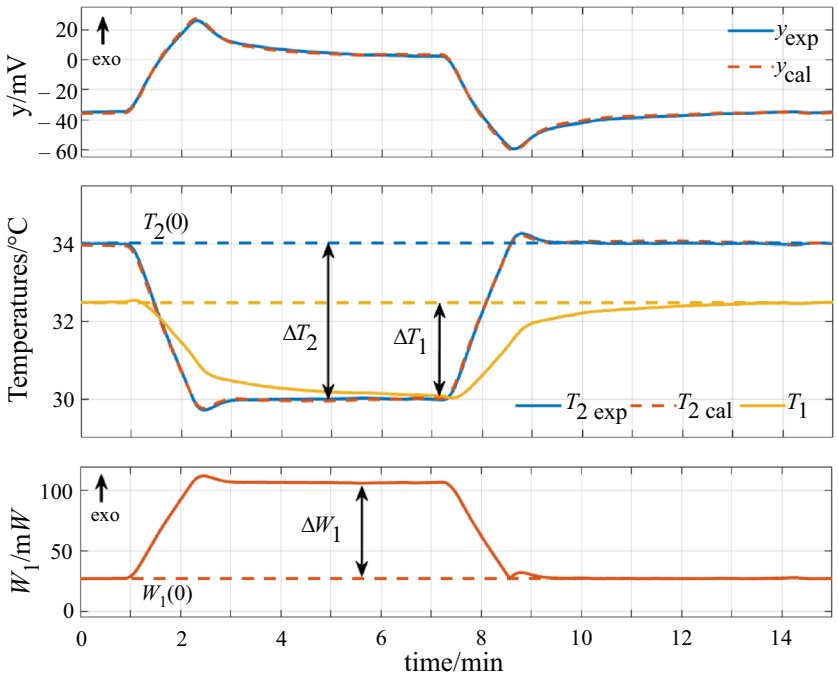

Fig. 1 Skin thermal properties measurement. The thermostat temperature T_2 is programmed to decrease from 34 to 30 °C. The calorimetric signal (y) and the thermostat temperature (T_2) are shown, including both experimental (exp) and modeled (cal) curves. The skin temperature (T_1) and heat flux (W_1) are also plotted

is performed by programming a linear variation of the thermostat temperature, while the subject is at rest. This mode is based on two assumptions: first, that the heat flux follows the same shape as the temperature change but with opposite sign (Eq. 4); and second, that the internal temperature remains constant during the excitation, allowing the internal skin thermal resistance to be defined as the change in skin temperature (ΔT_1) divided by the variation in skin heat flux (ΔW_1) (Eq. 5).

$$W_1(t) = W_1(0) - \Delta W_1 \frac{T_2(t) - T_2(0)}{\Delta T_2} \tag{4}$$

$$R_{skin} = \frac{\Delta T_1}{\Delta W_1} = \frac{\Delta T_2 + \Delta y/k}{\Delta W_1} \tag{5}$$

Figure 1 shows a measurement of this type, indicating the variables used in the calculation. The analysis is performed by fitting the experimental calorimetric signal and thermostat temperature to those obtained from the calorimetric model (Eq. 1), based on the assumptions previously described. The fitting process employs an iterative method based on the Nelder–Mead simplex algorithm, as modified by Lagarias et al. [20, 21]. This method minimizes the root mean squared error (RMSE) between the experimental and simulated signals.

This procedure fits both the transient and stationary states: the transient phase is used to estimate the heat capacity, while the steady-state phase allows to estimate the thermal resistance. The measured heat capacity mainly corresponds to the skin region affected by the calorimeter, together with the measurement plate, and its value depends on the thermal penetration depth of the excitation [20–25]. However, the accuracy of the thermal resistance estimation depends on the quality of the steady-state conditions achieved during measurement.

The second operating mode involves measuring the skin heat flux evolution over time. For this, the calorimeter is attached to the skin and the thermostat is maintained at a constant temperature. This mode is used when the subject is exercising. The measurement is non-invasive and performed on the skin region directly above the active muscle. This mode allows for the analysis of the muscle's thermal response during exercise, which is the main objective of this work.

Experimental

The same experimental protocol was followed for all measurements: each exercise session lasted 30 min, was performed on a stepper, and maintained a constant mechanical power of 80 W. The participant was a healthy 30-year-old male (90 kg, 1.78 m). Heart rate was monitored throughout the exercise, starting at an average of 85 beats per minute (bpm) and reaching a maximum of 165 bpm.

A skin calorimeter was placed on the rectus femoris of each thigh to assess the heat flux. During each session, the thermostat temperature was held constant and set to 28, 30, 32, 34, 36, or 38 °C in different trials. Ambient conditions were controlled, with an average room temperature of 23.4 ± 0.6 °C and relative humidity of average 45 ± 5%. Additional measurements were conducted before and

after the exercise to determine skin thermal properties by applying a thermostat temperature step of $\Delta T_2 = 4$ °C. Figure 2 illustrates the placement of the skin calorimeters on the thighs of the subject.

Analysis of the local heat loss during exercise

Transfer function approach

In all cases analyzed, it was possible to identify a transfer function (TF) between the mechanical power developed by the subject during exercise (W) and the heat flux measured by the skin calorimeter (W_1). This functional relationship exhibits a specific form that allows for an adequate fit during both the active exercise phase and the subsequent muscle recovery phase. The expression for this TF is given by Eq. 6:

$$\mathrm{TF}(s) = \frac{\Delta W_1(s)}{W(s)} = K\frac{1 + s\tau *}{(1 + s\tau)^2} \tag{6}$$

The TF is defined by a sensitivity K, representing the steady-state response to a unit step input, a double pole (s_1), and a zero (s^*_1), where $\tau = -1/s_1$ and $\tau^* = -1/s^*_1$. The fit between the experimental heat flux and the one generated by the TF model is performed by minimizing the RMSE between both curves, using the same fitting procedure than the one described above [20, 21]. The muscle can be modeled as a SISO (Single Input, Single Output) system. As described in the previous section, the input during the exercise phase is a positive step of 80 W, while for the post recovery phase, the same step is applied in the opposite direction.

Fig. 2 Placement of the calorimeters on the skin

Figure 3 shows the fitting for the cases in which the thermostat temperature (T_2) was 32 and 34 °C. Experimental heat flux (labeled "exp") is compared with the one obtained from the TF model (labeled "cal"). Additionally, the subject's heart rate is shown, which is fitted using a simple exponential function. The time constants associated with the heart rate during the exercise (τ_1) and recovery (τ_2) phases are also indicated. Figure 3 also shows the evolution of the local ambient temperature around the calorimeter (T_{01}). At the onset of exercise, the movement of the calorimeter induces a drop in this external temperature. The initial values of T_{01} were 25 and 26.7 °C for the $T_2 = 32$ °C and $T_2 = 34$ °C cases, respectively. The higher temperature in the second case is caused by the higher Peltier current, which was $I_{\mathrm{pel}} = 0.1$ A, compared to $I_{\mathrm{pel}} = 0.05$ A in the first case. This observation is consistent with Eq. 2. The obtained TF model parameters corresponding to the exercise and recovery phases, are shown in Table 2.

In all cases, the skin thermal resistance at the measurement site was determined before and after exercise, whit the subject at rest. This allows for an approximate estimation of the internal skin temperature using Eq. 7.

$$T_{\mathrm{int}} = T_1 + R_{\mathrm{skin}} W_1 = T_2 + y/k + R_{\mathrm{skin}} W_1 \tag{7}$$

Analogously to the heat flux analysis, a TF can be defined between the variation in internal temperature and the mechanical power developed during the exercise trial (Eq. 8). Table 3 presents the TF model parameters corresponding to the variation in internal temperature.

$$\mathrm{TF}(s) = \frac{\Delta T_{\mathrm{int}}(s)}{W(s)} = K\frac{1 + s\tau *}{(1 + s\tau)^2} \tag{8}$$

Simulations

Exercise stress tests in patients with cardiopulmonary conditions are designed to assess the response of the heart, lungs, and muscular system during exercise. These tests follow incremental protocols, commonly applied in sports medicine [26], and are adjusted to the patient's clinical condition to obtain reliable diagnostic results. In cardiac rehabilitation and related applications, exercise protocols are often performed at constant moderate workloads (60–80 W) [27].

Thus, the simulation as shown in Fig. 4 includes not only a step input (100 W), but also a ramp input (0–200 W over 20 min). In addition, although clinical stress tests usually last around 10 min, a duration of 20 min was chosen for the simulation, which is more appropriate to study local muscle thermal responses. On the other hand, we chose to simulate the internal temperature because it is more stable and relevant for physiologists.

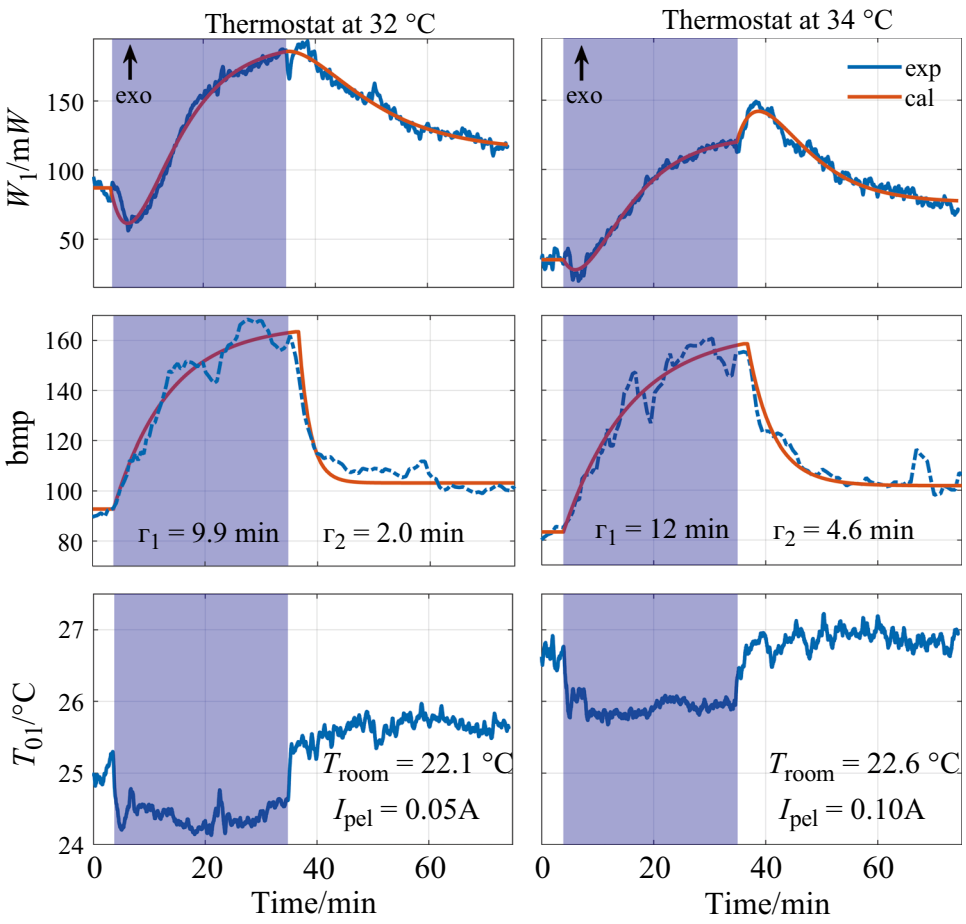

Fig. 3 Results of exercise measurements, performed in a stepper at constant 80 W mechanical power. Cases for thermostat temperatures of the calorimeters of 30 and 34 °C. Fit of the skin heat flux (W_1) using the TF model (Eq. 6); and heart rate (bpm) with simple exponentials. Blue curves correspond to experimental data and red to modeled ones. Local ambient temperature around the calorimeter (T_{01}) during the measurement is shown

Table 2 TF model parameters (Eq. 6) from heat flux measurements at different thermostat temperatures (T_2). ε is the Root Mean Squared Error of the fit (model vs. experimental signal)

T_2	Exercise			Recovery phase			
	K/mWW^{-1}	τ/s	τ*/s	K/mWW^{-1}	τ/s	τ*/s	ε/μW
28	0.7375	345.2	−338.0	0.5850	456.4	−476.3	68.1
30	1.3088	312.8	−228.1	1.3088	575.7	453.4	82.0
32	1.2937	345.4	−388.7	0.8887	518.7	−36.7	74.6
34	1.1075	357.5	−192.5	0.5363	359.0	−696.8	57.7
36	0.8787	322.9	−559.0	0.3825	425.7	−266.6	80.5
38	0.3975	456.5	−965.7	−0.4350	339.6	1366.5	60.2

Table 3 TF model parameters (Eq. 8) corresponding to the internal temperature at different thermostat temperatures (T_2). ε is the RMSE of the fit

T_2	Exercise			Recovery phase			
	K/mKW^{-1}	τ/s	τ*/s	K/mKW^{-1}	τ/s	τ*/s	ε/μK
28	31.2	345.2	−428.9	22.5	456.4	−666.0	2.7
30	53.7	312.8	−292.4	52.5	575.7	391.0	2.9
32	50.0	345.4	−429.2	32.5	518.7	−146.8	2.6
34	40.0	357.5	−253.4	17.5	359.0	−880.5	2.0
36	30.0	322.9	−662.2	11.2	425.7	−520.4	2.3
38	11.2	456.5	−1238.2	−17.5	339.6	1222.4	1.8

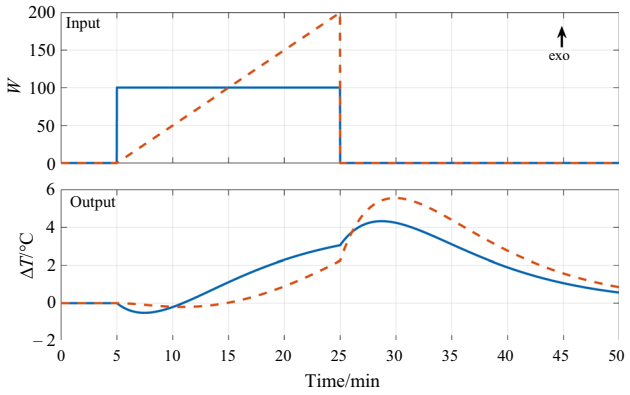

Fig. 4 Simulation of the increase in internal skin temperature (output) during and after exercise for two different exercise protocols (input). Step input cases (blue lines) and ramp input cases (red lines) are shown

For the simulations, the transfer function corresponding to $T_2 = 34$ °C was used (see Table 3). The simulation shows that the step protocol yields a higher signal-to-noise ratio, which makes TF identification more robust compared to the ramp protocol. However, for analyzing post-exercise thermal dynamics, the ramp protocol provides a better signal-to-noise ratio.

Discussion

A TF with three parameters is enough to describe both the static and dynamic thermal behavior of the working muscle during exercise, as shown by the fitting of the heat flux plots in Fig. 3 and the errors (ε) shown in Tables 2 and 3. This TF is of great interest in physiological studies, as it provides a quantitative representation of the underlying thermal processes. In this section, we discuss the role of each of the three parameters that characterize the thermal response, both for the heat flux and the internal temperature.

- The sensitivity (K) represents the increase in heat flux in response to a unit step of mechanical exercise, i.e., for 1 W of mechanical power. Experimental results show that this heat flux change slightly decreases as the thermostat temperature increases. This limitation highlights the importance of performing measurements under consistent thermal conditions (thermostat and ambient temperature and Peltier current) to ensure comparability. Additionally, an excessively high thermostat temperature can alter skin and muscle temperature and induce secondary thermal phenomena that may compromise the analysis, such as induced vasodilatation. Among the trials conducted, the case at $T_2 = 38°$ deviated from the uniformity observed in the other conditions. During the recovery phase, the sensitivity is consistently lower. This indicates that the muscle continues dissipating a heat flux higher than prior to exercise. Within the 1-h observation period, the body does not return to its original thermal state. This phenomenon has already been reported in the literature [28, 29].
- Regarding the dynamics, The TF includes a double pole characterized by the time constant τ, that defines the primary thermal response. For the case analyzed in this study, the average value was 5.6 min. The thermal response during exercise is consistently faster ($\tau_{mean} = 5.6$ min) than during recovery ($\tau_{mean} = 7.8$ min).
- The zero of the TF is characterized by τ^*, a negative parameter that defines the transient pulse consistently observed at the onset of exercise. This transient follows the form $a \cdot t \cdot e^{-t/\tau}$, where the amplitude a is given by $a = K \cdot (\tau^* - \tau)/\tau^2$. Since τ^* is negative, the resulting amplitude is also negative, leading to a negative initial transient in heat flux. This effect is attributed to the rapid change in muscle blood perfusion at the beginning of exercise [30, 31]. At the end of exercise, the heat flux decreases, and a second transient may occur, but in the opposite direction of the natural decay. This effect is not always evident and may be masked by a mismatch between the end of the exercise and the onset of heart rate recovery (note that the sign of τ^* may change during this phase). A slight delay in cardiovascular response can mask the thermal transient. This behavior depends on the specific exercise protocol. Notably, post-exercise transients are more pronounced in ramp than in step input protocols (Fig. 4).

Conclusions

This study illustrates the feasibility of skin calorimetry to non-invasively quantify local muscle heat loss during and after exercise, using a validated thermal model and a subject-muscle-specific transfer function (TF).

- Muscle heat flux during exercise and recovery can be described by a TF with three parameters (sensitivity, double pole, and zero), offering a physiologically meaningful representation of the thermal processes. Thermal sensitivity decreases with increasing thermostat temperature, highlighting the importance of maintaining consistent thermal conditions to ensure measurement comparability.
- In contrast, the average value of the time constant τ remained relatively stable across conditions, suggesting a possible link to a subject-specific physiological characteristics. Additionally, it was observed that post-exercise heat flux does not return to baseline within 1 h, indicating prolonged thermal dissipation by the muscle, in agreement with previous findings.

- Thermal characterization of muscle using TF enables relevant simulations, allowing the analysis of thermal effects and the design of personalized exercise protocols.

Two main limitations of this study should be noted. First, the analysis was based on a single subject, highlighting the need for additional measurements in a broader population. Second, the potential effect of sweating must be considered, as it might reduce the heat flux to the measuring device during exercise. Further research involving a larger population and the development of modeling strategies to account for evaporative losses is needed. Despite these limitations, the model is published at this stage as a reference point for subsequent simulations and experimental validation.

Author contributions Conceptualization was contributed by PJRdR and MRdR; methodology, investigation, and visualization were involved by PJRdR; software, formal analysis, writing—original draft preparation, and writing—review and editing were performed MRdR; validation was done FS, MRdR (Miriam Rodríguez de Rivera), and PJRdR; resources and supervision were responsible by FS; data curation and project administration were done by MRdR (Miriam Rodríguez de Rivera); All authors have read and agreed to the published version of the manuscript.

Funding This research was funded by the Government of the Canary Islands through the "Convocatoria 2024 de Subvenciones para la realización de Proyectos de I+D Aplicada (Modalidad B), en el marco de la Estrategia de Especialización Inteligente de Canarias RIS-3 Ampliada, y cofinanciado por el Fondo Europeo de Desarrollo Regional (FEDER) 2021–2027" Project: "Monitorización de la capacidad calorífica y la resistencia térmica de la piel mediante un calorímetro de piel (SKINCAL)" ID: ProID2024010002.

Declarations

Conflict of interest The authors declare that they have no known competing financial interests or personal relationships that could have appeared to influence the work reported in this paper.

Ethical approval The study was conducted in accordance with the Declaration of Helsinki and approved by the Human Experimentation Ethical Committee of the University of las Palmas de Gran Canaria (protocol code CEIH-2024-02, approved on April 2024).

Informed consent. Informed consent was obtained from all subjects involved in the study.

References

1. Böning D, Maassen N, Steinach M. The efficiency of muscular exercise. Dtsch Z Sportmed. 2017. https://doi.org/10.5960/dzsm.2017.295.
2. Ettema G, Lorås HW. Efficiency in cycling: a review. Eur J Appl Physiol. 2009. https://doi.org/10.1007/s00421-009-1008-7.
3. Gaesser GA, Brooks GA. Muscular efficiency during steady-rate exercise: effects of speed and work rate. J Appl Physiol. 1975. https://doi.org/10.1152/jappl.1975.38.6.1132.
4. Alonso JG, Teller C, Andersen SL, Jensen FB, Hyldig T, Nielsen B. Influence of body temperature on the development of fatigue during prolonged exercise in the heat. J Appl Physiol. 1999. https://doi.org/10.1152/jappl.1999.86.3.1032.
5. Delsoglio M, Achamrah N, Berger MM, Pichard C. Indirect calorimetry in clinical practice. J Clin Med. 2019. https://doi.org/10.3390/jcm8091387.
6. Ferrannini E. The theoretical bases of indirect calorimetry: a review. Metabolism. 1988. https://doi.org/10.1016/0026-0495(88)90110-2.
7. Masur L, Brand F, Düking P. Response of infrared thermography related parameters to (non-)sport specific exercise and relationship with internal load parameters in individual and team sport athletes—a systematic review. Front Sports Act Living. 2024. https://doi.org/10.3389/fspor.2024.1479608.
8. Ramirez-Garcia Luna JL, Rangel-Berridi K, Bartlett R, Fraser RDJ, Martínez-Jiménez MA. Use of infrared thermal imaging for assessing acute inflammatory changes: a case series. Cureus. 2022. https://doi.org/10.7759/cureus.28980.
9. Perrey S, Quaresima V, Ferrari M. Muscle oximetry in sports science: an updated systematic review. Sports Med. 2024. https://doi.org/10.1007/s40279-023-01987-x.
10. Daanen HAM, Kohlen V, Teunissen LPJ. Heat flux systems for body core temperature assessment during exercise. J Therm Biol. 2023. https://doi.org/10.1016/j.jtherbio.2023.103480.
11. de Rivera PJ, de Rivera M, Socorro F, de Rivera M. Heat flow measurement of human skin using a calorimetric sensor with a programmable thermostat. An alternative to climate chambers. Measurement. 2021;201:111693. https://doi.org/10.1016/j.measurement.2022.111693.
12. Kenny GP, Reardon FD, Zaleski W, et al. Muscle temperature transients before, during, and after exercise measured using an intramuscular multisensor probe. J Appl Physiol. 2003. https://doi.org/10.1152/japplphysiol.01107.2002.
13. de Rivera PJ, de Rivera M, Socorro F, Callicó GM, Calbet JAL, de Rivera M. Heat flow, heat capacity and thermal resistance of localized surfaces of the human body using a new calorimetric sensor. J Therm Anal Calorim. 2022;147(13):7385–98. https://doi.org/10.1007/s10973-021-11062-0.
14. de Rivera M, de Rivera PJ. New optimized skin calorimeter version for measuring thermal responses of localized skin areas during physical activity. Sensors. 2024;24:5927. https://doi.org/10.3390/s24185927.
15. Wang H, Burgei W, Zhou H. Analytical solution of one-dimensional Pennes' bioheat equation. Open Phys. 2020. https://doi.org/10.1515/phys-2020-0197.
16. Brown A, Marshall TK. Body temperature as a means of estimating the time of death. Forensic Sci. 1974. https://doi.org/10.1016/0300-9432(74)90093-4.

17. Waterman FM. Estimation of temperature artifact from a short interruption in ultrasonic power. Int J Hyperthermia. 1992. https://doi.org/10.3109/02656739209021793.
18. Subramaniam JS, Hubig M, Muggenthaler H, et al. Sensitivity of temperature-based time since death estimation on measurement location. Int J Legal Med. 2023. https://doi.org/10.1007/s00414-023-03040-y.
19. de Rivera PJ, de Rivera M, Socorro F, de Rivera M. Modeling skin thermal behavior with a cutaneous calorimeter: local parameters of medical interest. Modelling. 2025. https://doi.org/10.3390/modelling6020042.
20. Nelder JA, Mead R. A simplex method for function minimization. Comput J. 1965. https://doi.org/10.1093/comjnl/7.4.308.
21. Lagarias JC, Reeds JA, Wright MH, Wright PE. Convergence properties of the Nelder–Mead simplex method in low dimensions. SIAM J Optim. 1998. https://doi.org/10.1137/S1052623496303470.
22. de Rivera PJ, de Rivera M, Socorro F, de Rivera M. Study of the thermal measurement depth of a skin calorimeter using simple RC and TF models. Int J Heat Mass Transf. 2025. https://doi.org/10.1016/j.ijheatmasstransfer.2024.126256.
23. Van de Staak WJBM, et al. Measurements of the thermal conductivity of the skin as an indication of skin blood flow. J Invest Dermatol. 1968. https://doi.org/10.1038/jid.1968.107.
24. Webb RC, Pielak RM, Bastien P, Ayers J, et al. Thermal transport characteristics of human skin measured in vivo using ultrathin conformal arrays of thermal sensors and actuators. PLoS ONE. 2015. https://doi.org/10.1371/journal.pone.0118131.
25. Tian L, Li Y, Webb RC, et al. Flexible and stretchable 3ω sensors for thermal characterization of human skin. Adv Funct Mater. 2017. https://doi.org/10.1002/adfm.201701282.
26. Bourgois G, Colosio AL, Caen K, Bourgois JG, Mucci P, Boone J. The effect of acute heat exposure on the determination of exercise thresholds from ramp and step incremental exercise. Eur J Appl Physiol. 2023. https://doi.org/10.1007/s00421-022-05106-y.
27. Dibben G, Faulkner J, Oldridge N, Rees K, Thompson DR, Zwisler AD, et al. Exercise-based cardiac rehabilitation for coronary heart disease. Cochrane Database Syst Rev. 2021. https://doi.org/10.1002/14651858.cd001800.pub4.
28. Chaillou T, Treigyte V, Mosely S, Brazaitis M, Venckunas T, Cheng AJ. Functional impact of post-exercise cooling and heating on recovery and training adaptations: application to resistance, endurance, and sprint exercise. Sports Med Open. 2022. https://doi.org/10.1186/s40798-022-00428-9.
29. Freitag L, Clijsen R, Deflorin C, Taube W, Taeymans J, Hohenauer E. Intramuscular temperature changes in the quadriceps femoris muscle after post-exercise cold-water immersion (10 °C for 10 min): a systematic review with meta-analysis. Front Sports Act Living. 2021. https://doi.org/10.3389/fspor.2021.660092.
30. Kellogg DL, Johnson JM, Kosiba WA. Competition between cutaneous active vasoconstriction and active vasodilation during exercise in humans. Am J Physiol. 1991. https://doi.org/10.1152/ajpheart.1991.261.4.H1184.
31. Simmons GH, Wong BJ, Holowatz LA, Kenney WL. Changes in the control of skin blood flow with exercise training: where do cutaneous vascular adaptations fit in? Exp Physiol. 2011. https://doi.org/10.1113/expphysiol.2010.056176.